Spatiotemporal periodic pattern and propagated spatiotemporal on-off intermittency in the one-way coupled map lattice system

Fagen Xie [1,2] and Gang Hu [3]
[1] China Center of Advanced Science and Technology (World Laboratory), P.O. Box 8730, Beijing 100080, China
[2] Institute of Theoretical Physics, Academia Sinica, Beijing 100080, China
[3] Department of Physics, Beijing Normal University, Beijing 100875, China
(Received 7 November 1995)

One-way coupled map lattice system is investigated. An antiphase spatiotemporal period-2 state (a running wave), and an alternative type of propagated spatiotemporal on-off intermittency are found. The stability of the wave is discussed in both stationary frame and comoving frame. They are characterized by conventional Lyapunov exponent and comoving Lyapunov exponent, respectively. The stability boundaries of this state are also obtained in the parameter plane. Numerical calculation shows that the propagated spatiotemporal on-off intermittency has negative Lyapunov exponent. The distribution of the laminar phases for various sites is calculated numerically. Those sites far from the boundary site obey a power law with power exponent $-3/2$. This interesting phenomenon seems to be independent of the choices of local function map.

PACS number(s): 05.45.+b

I. INTRODUCTION

In recent decades, many interesting investigations have been shifted to the complex spatiotemporal behaviors in the extended systems in optics, fluid, biology, etc. These systems exhibit very rich phenomenology including a wide variety of both spatial and temporal periodic structures, solitions, traveling waves, domain walls, intermittency, chaos, developed turbulence, etc. Coupled map lattices (CMLs), which are introduced as simple models showing the essential features of spatiotemporal systems, have attracted great interest. The CMLs with the nearest-neighbor symmetric coupling has been most extensively investigated [1–10]. However, recently the interest in one-way coupled map lattice models (OCMLs) has increased [11–16]. This OCML model is closely related to physical open flow systems, and therefore, is important for investigating the behaviors of turbulence, pipe flow, and traffic flow [17,18].

Specifically, the OCML is defined as

$$x_{n+1}(i)=(1-\epsilon)f[x_n(i)]+\epsilon f[x_n(i-1)], \quad i=0,1,2,\ldots, \tag{1}$$

where n, i, and ϵ are the discrete time step, the lattice site index, and the coupling coefficient, respectively. The local mapping function $f(x)$ is chosen to be the logistic map $f(x)=ax(1-x)$, where a is the nonlinear parameter. Previous studies in this model often chose a fixed boundary condition, i.e., the first site ($i=0$) always stays at a fixed point. In this paper we study two cases of boundary conditions. The results will show a strong dependence on the boundary condition. The system (1) possesses many interesting features, such as spatial period doubling, comoving instability, and the selective amplification of small noise [11–14]. The regions for various spatiotemporal patterns were classified in the phase diagram (a,ϵ) [15]. In Ref. [6] Qu and Hu revealed a globally stable period-2 running wave for CMLs with diffusion coupling. In Ref. [16] this state is also found for open systems. However, detailed discussions about this state have not been given. In this paper we focus our attention on this interesting parameter region. The boundary condition is chosen as (a) the fixed point of local function maps, i.e, $x(0)\equiv 1-1/a$, and (b) the above period-2 state. We denote the spatial period-k state as Sk, and temporal period m state as Tm, thus the spatiotemporal period-2 state is denoted as $S2T2$.

This paper is organized as follows. In Sec. II, we analytically reveal the existence of the spatiotemporal period-2 state, its stability boundaries, and some interesting spatiotemporal bifurcations from this state. In Sec. III, we investigate a different type of intermittency, the so called propagated spatiotemporal on-off intermittency. Finally, the conclusion is given in Sec. IV.

II. SPATIOTEMPORAL PERIOD-2 STATE, STABILITY BOUNDARIES, AND BIFURCATIONS

The $S2T2$ state is an antiphase state both for time and space. Thus we assume the state has the form (x_+x_-,x_-x_+). Then the system (1) becomes

$$\begin{aligned} x_+&=(1-\epsilon)f(x_-)+\epsilon f(x_+),\\ x_-&=(1-\epsilon)f(x_+)+\epsilon f(x_-), \end{aligned} \tag{2}$$

which can be solved as

$$\begin{aligned} x_\pm=&\frac{1+a-2a\epsilon}{2a(1-2\epsilon)}\\ &\pm\frac{\sqrt{(1+a-2a\epsilon)^2-4(1-a)(1-\epsilon)-8a(1-\epsilon)^2}}{2a(1-2\epsilon)}. \end{aligned} \tag{3}$$

These solutions exist only in the parameter region

$$a\geqslant 2+\frac{1}{1-2\epsilon} \quad \text{or} \quad \epsilon\leqslant\frac{a-3}{2(a-2)}. \tag{4}$$

When the first site ($i=0$) is fixed to the fixed point $x_n(0)=1-1/a$, the behaviors of the several sites near the boundary site are very interesting and complicated. With variation of a and ϵ, these sites may exhibit periodic and chaotic motions. But the deviation of site's state from the $S2T2$ state exponentially decays as the site index increases.

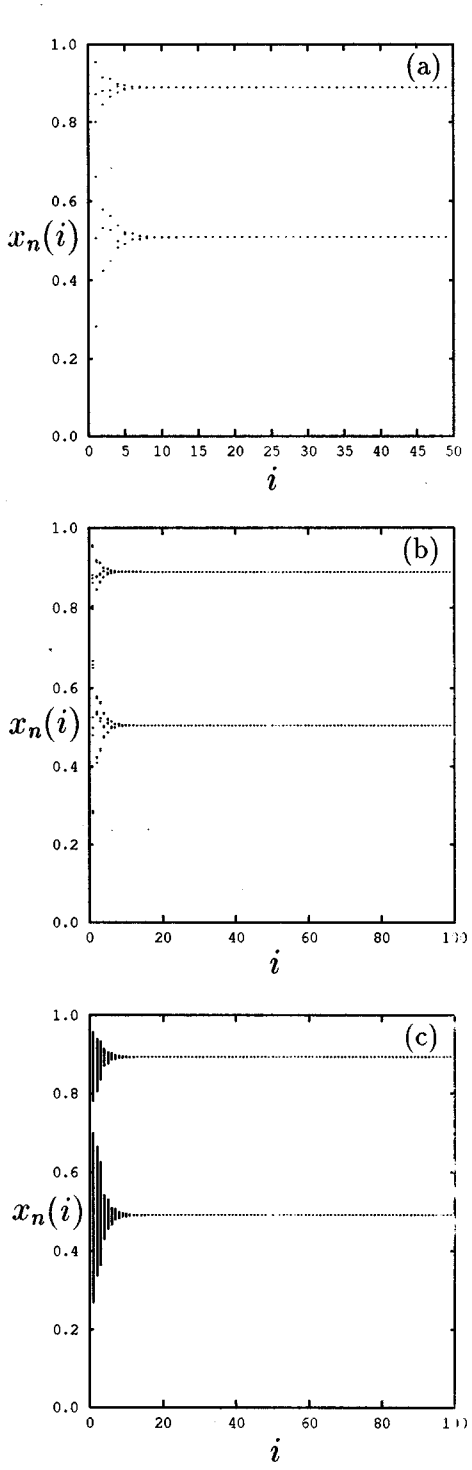

FIG. 1. The time-space structure of the system for various ϵ and $a=4$. The boundary condition is chosen as fixed point $x_n(0)\equiv 1-1/a$. The boundary condition in the following figures is the same as Fig. 1 except for Fig. 5. (a) $\epsilon=0.185$. (b) $\epsilon=0.183$. (c) $\epsilon=0.174$.

These features are clearly shown in Fig. 1. In Fig. 2 we show various bifurcations of some sites versus ϵ for $a=4$. Although the sites near the fixed boundary site may manifest different behaviors according to the control parameter, the sites far from the fixed boundary site ($i\geqslant 20$) always stay at the $S2T2$ state. As the boundary condition is chosen at this exact period-2 solution, the above bifurcations disappear, and the whole system is set at the $S2T2$ state in the parameter regions of Figs. 1 and 2.

In an open flow system, the instability of a state (or a pattern) can be referred to as the stationary instability and the comoving instability. The stationary instability is characterized by conventional Lyapunov exponents, which can be immediately found as the eigenvalues of the product of Jacobi matrices

$$\lambda(i)=\ln(1-\epsilon)+\lim_{n\to\infty}\frac{1}{n}\sum_{k=1}^{n}\ln|f'[x_k(i)]|, \tag{5}$$

where i is the lattice site index and the prime denotes the derivative of the function. Due to the fact that the upper triangle Jacobi matrix elements are zero for the system (1), there is no coupling in the expression of $\lambda(i)$ and the ith exponent characterizes the local motion of the ith site. For the $S2T2$ state, the largest Lyapunov exponent is given as

$$\lambda=\ln(1-\epsilon)+\tfrac{1}{2}\ln|f'(x_+)f'(x_-)|, \tag{6}$$

where x_+ and x_- are given by Eq. (3). If $\lambda<0$, the $S2T2$ state is stable with respect to the stationary frame. However, this stability can't completely guarantee the state's stability. The so-called comoving instability should also be taken into account. This instability is characterized by the comoving Lyapunov exponent, which is defined as

$$L(v,i)=\lim_{\delta x_0(i)\to 0}\lim_{n\to\infty}\frac{1}{n}\ln\left|\frac{\delta x_n(i+[nv])}{\delta x_0(i)}\right|, \tag{7}$$

where $[nv]$ denotes the largest integer equal to or smaller than nv. $L>0$ means that the small perturbation of the ith site can be amplified at time n on the site $i+[nv]$. Usually, the comoving Lyapunov exponent is independent of the site. However, being influenced by the fixed boundary condition, the comoving Lyapunov exponents of the several sites near the boundary site ($i=0$) are different from other, but these exponents quickly tend to the same asymptotic value as the site index increases. This feature is shown in Fig. 3 at $a=4$, and $\epsilon=0.174$. The asymptotic comoving Lyapunov exponent of the $S2T2$ state is given by

$$L(v)=\tfrac{1}{2}\ln|f'(x_+)f'(x_-)|+\frac{v}{2}\ln\left|\frac{f'(x_+)}{f'(x_-)}\right|+(1-v)\ln(1-\epsilon)$$
$$+v\ln\frac{\epsilon}{v}+\frac{v}{2}\ln\frac{1-v^2}{4}+\tfrac{1}{2}\ln\frac{1+v}{1-v}. \tag{8}$$

The derivation of Eq. (8) is given in the Appendix. The exponent is a function of the propagation velocity. When the velocity v is

$$v_0 = \left[1+4\left|\frac{f'(x_-)}{f'(x_+)}\right|\frac{(1-\epsilon)^2}{\epsilon^2}\right]^{-1/2}, \tag{9}$$

the comoving Lyapunov exponent takes maximum as

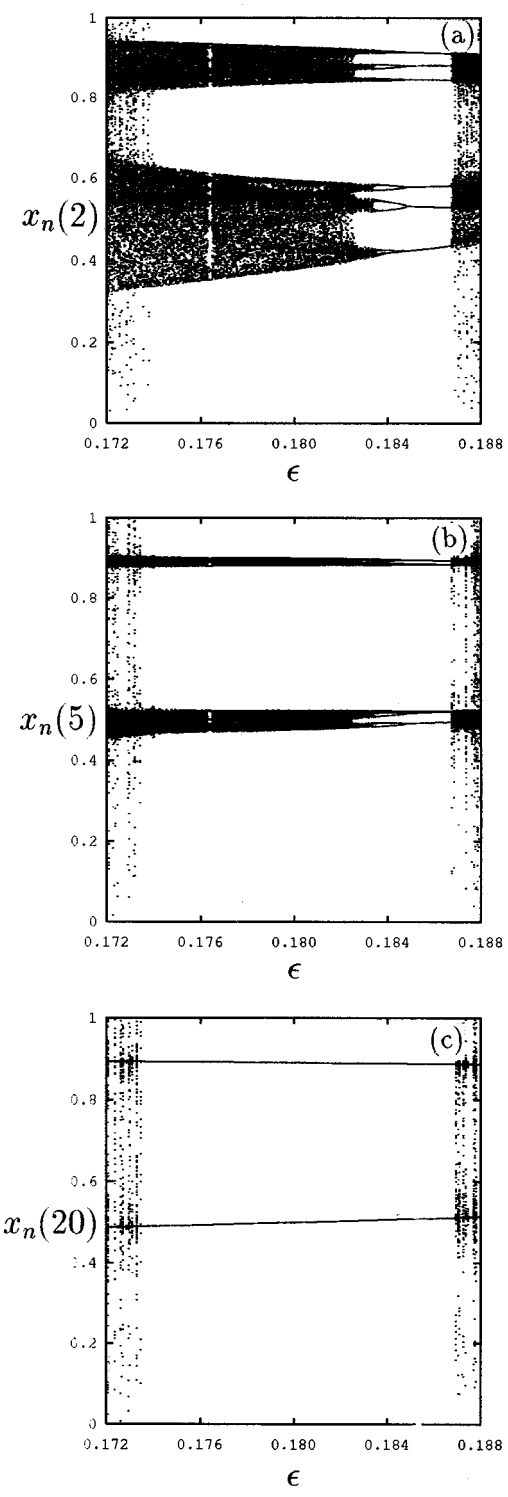

FIG. 2. The asymptotic state versus ϵ for some sites at $a=4$. (a) $i=2$. (b) $i=5$. (c) $i=20$.

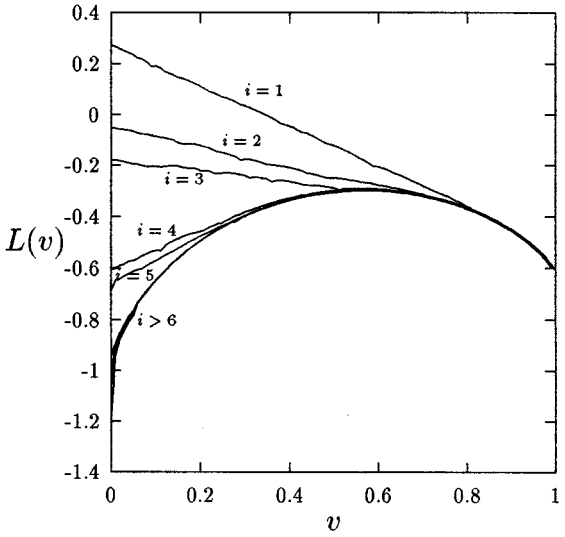

FIG. 3. The comoving Lyapunov exponents versus v for $a=4$ and $\epsilon=0.174$.

$$L_{\max}=\tfrac{1}{2}\ln|f'(x_+)f'(x_-)|+\frac{v_0}{2}\ln\left|\frac{f'(x_+)}{f'(x_-)}\right| + (1-v_0)\ln(1-\epsilon)+v_0\ln\frac{\epsilon}{v_0} + \frac{v_0}{2}\ln\frac{1-v_0^2}{4}+\frac{1}{2}\ln\frac{1+v_0}{1-v_0}. \tag{10}$$

As $L_{max}<0$, the $S2T2$ state is absolutely stable in both stationary ($v=0$) and the comoving frames. Therefore, neglecting the influence of boundary condition, the stability boundaries of the $S2T2$ state are given by the zero maximum comoving Lyapunov exponent, i.e,

$$L_{max}=0. \tag{11}$$

The comoving stability boundaries are shown in Fig. 4 by the dashed lines. When we change the upper control parameters by crossing the upper dashed line the system undergoes spatiotemporal intermittency. But when we go down by crossing the lower dashed line the system undergoes spatial period-doubling bifurcation along the site-index-increasing direction. The solid lines in Fig. 4 show the critical stability boundaries of a propagated spatiotemporal on-off intermittency for the fixed boundary condition. We will discuss this very interesting phenomenon in the next section. The stability region of the $S2T2$ state depends on boundary condition. The upper solid line is lower than the dashed one. However, the lower dashed and solid lines intersect at the parameter point $a\approx3.925$, $\epsilon\approx0.144$. As $a>3.925$, the solid line is above the dashed one, but the dashed line is above the solid one for $a<3.925$. Therefore, totally, in the case of fixed boundary condition, the stability region of the $S2T2$ state is margined by the upper solid line, the lower dashed line for $a<3.925$, and the lower solid line for $a>3.925$. It is emphasized that for fixed boundary condition the $S2T2$ state may lose its stability via on-off intermittency even when it is

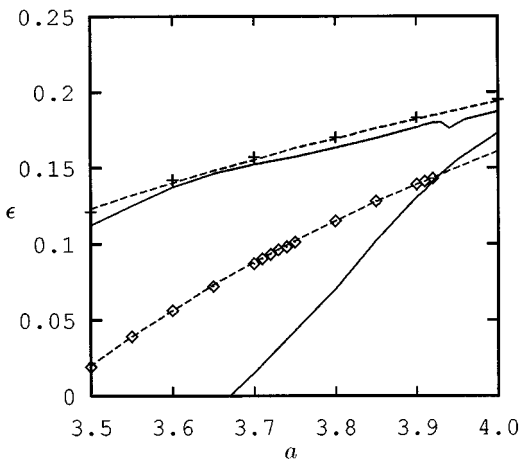

FIG. 4. The comoving stability boundaries of the $S2T2$ state (dashed lines) and the critical propagated spatiotemporal on-off intermittency boundaries (solid lines) in the parameter plane (a,ϵ). For the fixed boundary condition, the stability region of the $S2T2$ state is margined by the upper solid lines, the lower dashed line for $a<3.925$, and the lower solid one for $a>3.925$. The stability boundaries of the $S2T2$ state is completely given by the dashed lines for the period-2 boundary condition.

stable in a comoving frame for arbitrary velocity. The reason is that the chaotic impact from the sites near the boundary site may totally change the property of the motions of sites down string far from the left boundary site. In the case of period-2 boundary condition, the stability boundaries of this $S2T2$ state are completely decided by the dashed lines since there is no chaotic impact from the sites near the boundary site, and no on-off intermittency appears. The analytic results are in good agreement with the numerical calculations, which are shown by the diamonds and pluses. For the period-2 boundary condition some beautiful and interesting bifurcations are exhibited in Fig. 5 after the $S2T2$ state loses its stability.

III. PROPAGATED SPATIOTEMPORAL ON-OFF INTERMITTENCY

In the fixed boundary condition case, the sites near the boundary site exhibit periodic or chaotic motions (see Fig. 1), but the behavior quickly tends to that of the $S2T2$ state as the site index is large ($i\geqslant 20$). For $a=4$ and $\epsilon=0.174$, these near-boundary sites move in two chaotic bands. This two chaotic bands exponentially decay to the $S2T2$ quickly as the distance of the given site from the boundary site increases. The envelope of the whole system is fixed after the transient process (as shown in Fig. 1). Except for a few sites near the boundary site, the distances between the envelope and the corresponding period-2 positions decay exponentially as

$$\mathbf{\Delta r}(i)=\mathbf{A}e^{-\beta i}, \tag{12}$$

where $\mathbf{\Delta r}(i)=[\mathbf{\Delta r}_+(i),\mathbf{\Delta r}_-(i)]$ are the ith site's maximum deviations from the period-2 state $[\mathbf{x_0}=(x_+,x_-)]$. The $\mathbf{A}=(A_+,A_-)$ depends on the boundary condition. The decay exponent β depends on the parameters a and ϵ. This exponent can be worked out analytically as follows. First as the site is far away from the boundary site $(i=0)$, the deviations around the period-2 state are very small, and linearization around this state is valid. In the linear case the margin certainly maps to margin itself. Therefore, the envelope is a

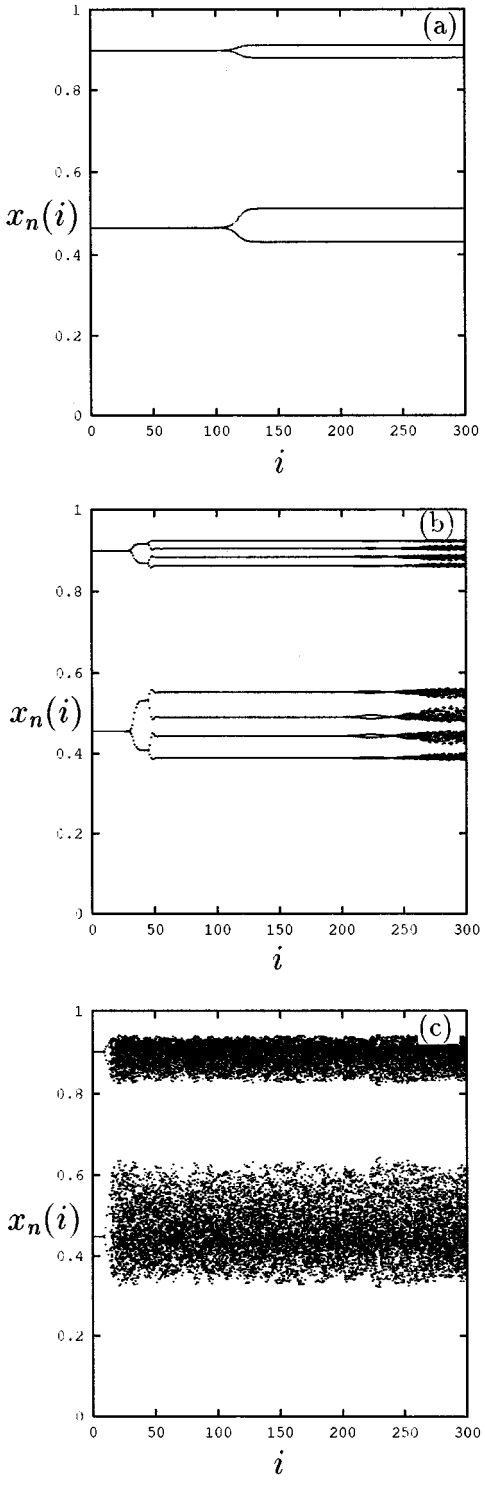

FIG. 5. The time-space structure of the system for $a=4$ and various ϵ in the case of period-2 boundary condition. (a) $\epsilon=0.155$. (b) $\epsilon=0.147$. (c) $\epsilon=0.141$.

stationary period-4 state. By inserting Eq. (12) into the linearized Eq. (1), we immediately get

$$a(1-\epsilon)(1-2x_-)A_- - [a\epsilon(1-2x_+)e^{\beta}+1]A_+ = 0,$$
$$[a\epsilon(1-2x_-)e^{\beta}+1]A_- + a(1-\epsilon)(1-2x_+)A_+ = 0. \tag{13}$$

Since A_- and A_+ are nonzero values, Eq. (13) leads to the condition

$$\begin{vmatrix} a(1-\epsilon)(1-2x_-) & -[a\epsilon(1-2x_+)e^{\beta}+1] \\ [a\epsilon(-1-2x_-)e^{\beta}+1] & a(1-\epsilon)(1-2x_+) \end{vmatrix} = 0. \tag{14}$$

From the above determinant, β can be calculated. At $a=4$

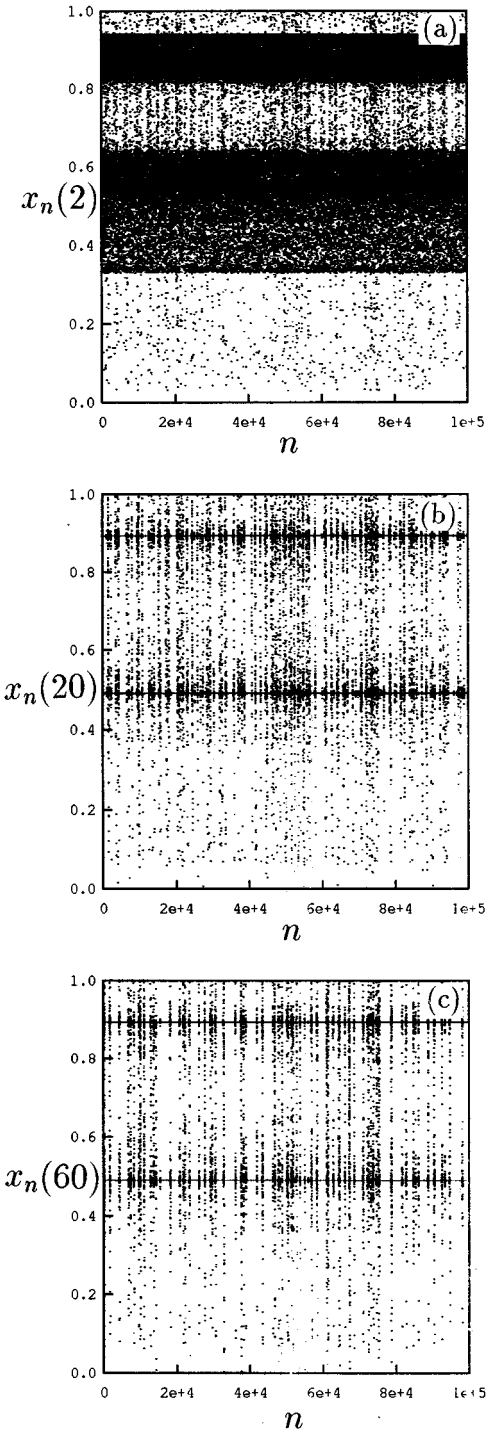

FIG. 6. The time evolutions of some sites for $a=4$ and $\epsilon=0.173$. (a) $i=2$. (b) $i=20$. (c) $i=60$.

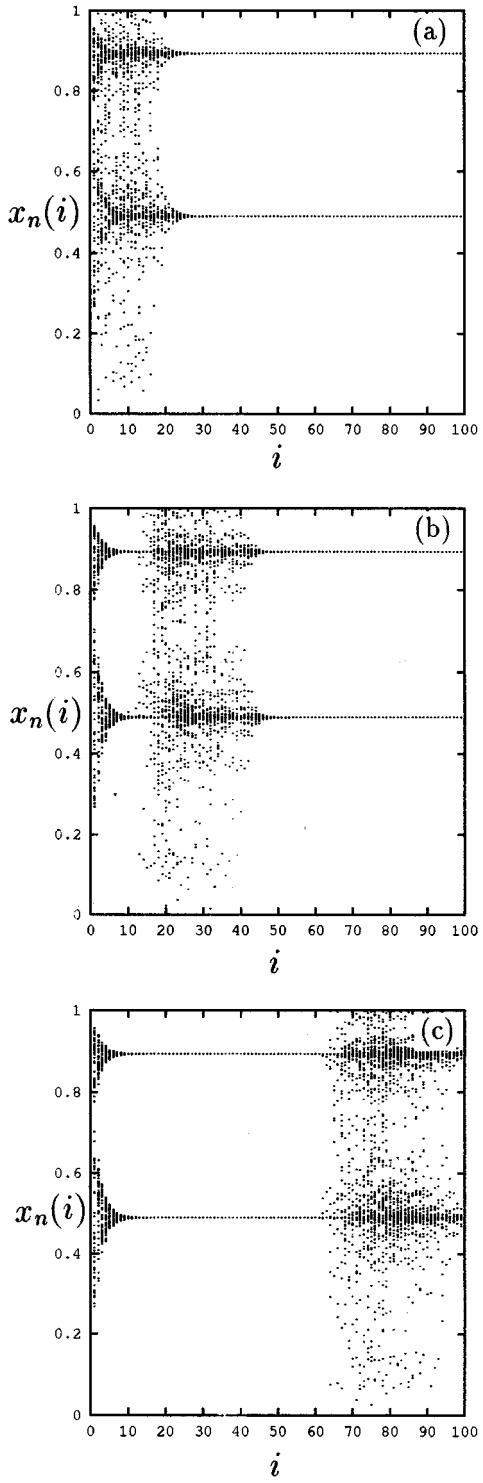

FIG. 7. $x_n(i)$ data plotted in 100 iterations at $a=4$ and $\epsilon=0.173$. The plotted iterations are from $n=6300$ to $n=6400$ for (a), $n=7000$ to $n=7100$ for (b), and $n=7300$ to $n=7400$ for (c).

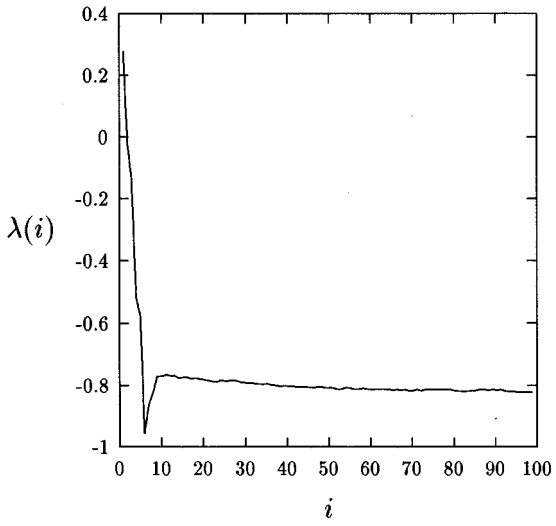

FIG. 8. The Lyapunov exponent versus the site index at $a=4$, $\epsilon=0.173$.

and $\epsilon=0.174$, we have $x_+=0.892\,503$, $x_-=0.490\,932$, and then obtain $\beta\approx 0.45$, which is confirmed by numerical calculations.

As we change the parameters a and ϵ to some critical values, the behavior of the system suddenly changes. The exponential decay law is broken. The critical values of ϵ are 0.1737 and 0.1870 for $a=4$. As ϵ increases over the threshold 0.187, or decreases below the threshold 0.1737, the behavior of the third site ($i=2$) suddenly changes, random bursts continuously generate from the two chaotic bands [see Fig. 6(a)]. This is nothing but the characteristic of crisis-induced intermittency, i.e., a phase transition from local two chaotic bands to a single chaotic band covering the entire interval (0,1). Since the system is one-way coupled, these random bursts generated from the third site quickly propagate to right. The sites far away from the boundary site display the characteristic of on-off intermittency. They stay at the period-2 state (''off'' state) for a very long time, suddenly depart quickly from and then return quickly to the off state. The time evolutions of sites $i=20$ and 60 are shown in Figs. 6(b) and 6(c) for $a=4.0$ and $\epsilon=0.173$. The features of on-off intermittency are clear. The propagation feature of this intermittency is shown in Fig. 7. The moving velocity is about the order of ϵ. The Lyapunov exponents of the system are shown in Fig. 8 for the same parameters. It is obvious that the Lyapunov exponents of the far-distance sites are all negative at this spatiotemporal on-off intermittency, showing that the $S2T2$ state is comovingly stable at the given parameters, and the instability is associated to the large scale chaotic impact from near-boundary sites.

In order to characterize the statistical property of this spatiotemporal intermittency, we calculate, numerically, the distribution probability P_n of the laminar phases shown in Fig. 9 for some sites at $a=4$ and $\epsilon=0.173$. A total of 10^8 iterations of Eq. (1) were computed to obtain these curves. The threshold for the laminar phase was defined by

$$|x(i)-x_0|<\tau=10^{-3}, \tag{15}$$

where, $x_0=(x_+,x_-)$. P_n represents the probability of the laminar phase of length n, namely $P_n=M_n/N$, where N is the total number of segments of the laminar phase, and M_n is the number of those of length n. As a site is far away from the boundary site, the distribution tends to the asymptotic distribution, which is characterized by a power law with power exponent $-3/2$. It is interesting to emphasized that this critical distribution is ''self-organized'' from propagation since the sites near the boundary site, which generates the bursts, don't possess this power law behavior (for $i=20$, the deviation from the $-3/2$ power law is already clearly observed, for $i<20$ the exponential decay law more and more prevails as i decreases).

The critical boundaries of this propagated spatiotemporal on-off intermittency in the parameter plane are shown in Fig. 4 with solid lines.

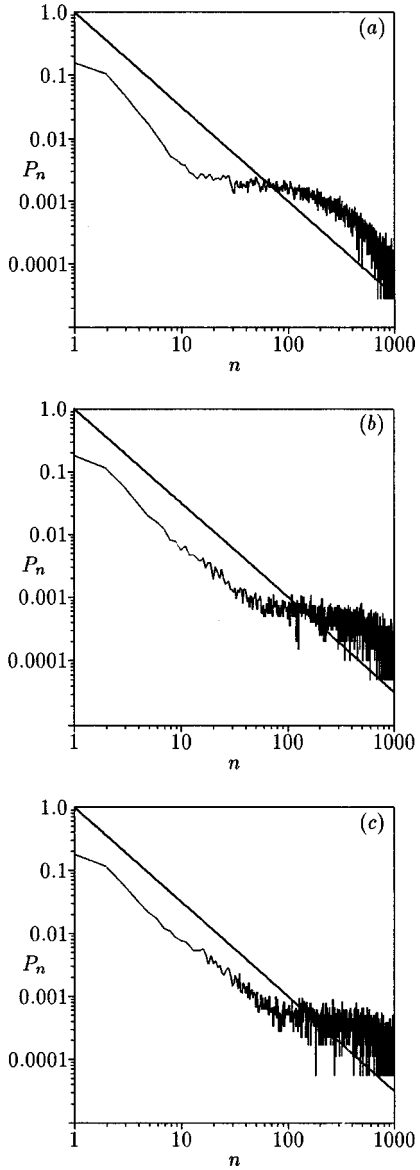

FIG. 9. The distributions P_n of laminar phases for several sites at $a=4$, $\epsilon=0.173$. The solid line is the perfect-3/2 power law decay. (a) $i=20$. (b) $i=60$. (c) $i=80$.

IV. CONCLUSION

One-way coupled map lattice system is closely related to the physical open flow system. We have studied some interesting dynamical behaviors of this system from both analytic and numerical calculations.

First, we have worked out the spatiotemporal period-2 state in the weak coupling region. This state is anti-phase in both time and space. Stability of this state has been analyzed in both stationary frame and comoving frame. The conventional Lyapunov exponent and the comoving Lyapunov exponent are solved analytically for the $S2T2$ state. The stability boundaries of this state are obtained. In open flow systems the comoving Lyapunov exponent plays an important role.

Second, we have found a different type of intermittency in this systems, the so called propagated spatiotemporal on-off intermittency. This intermittency is a global behavior of the extended system. The crisis behavior of the sites near the boundary site results in this interesting phenomenon. Furthermore, as the sites are far away from the fixed boundary site, the laminar phases obey uniquely distribution. This distribution is characterized by a power law with exponent $-3/2$. By tests with several models we found that all features are independent of the choices of local function map. They are universal properties. We believe this intermittency can be experimentally verified in the actual physical open flow systems.

ACKNOWLEDGMENTS

This work was supported partially by the Chinese Natural Science Foundation, Project Nonlinear Science, and the Open Laboratories Project of Academia Sinica.

APPENDIX

Let us consider the evolution induced by a small disturbance applied on the lattice site i, i.e., $\delta x_0(i)$, then we have for the first iteration,

$$\delta x_1(i)=(1-\epsilon)f'(x_0(i))\delta x_0(i),$$

$$\delta x_1(i+1)=\epsilon f'(x_0(i))\delta x_0(i), \tag{A1}$$

the others are zero. The second iteration follows as

$$\delta x_2(i)=(1-\epsilon)^2 f'(x_1(i))f'(x_0(i))\delta x_0(i),$$

$$\begin{aligned}\delta x_2(i+1)=(1-\epsilon)\epsilon[&f'(x_1(i+1))f'(x_0(i))\\&+f'(x_1(i))f'(x_0(i))]\delta x_0(i),\end{aligned} \tag{A2}$$

$$\delta x_2(i+2)=\epsilon^2 f'(x_1(i+1))f'(x_0(i))\delta x_0(i),$$

the others are zero.

The nth iteration follows as

$$\delta x_n(i)=(1-\epsilon)^n\prod_{k=0}^{n-1} f'(x_k(i))\delta x_0(i),$$

$$\delta x_n(i+p)=(1-\epsilon)^{n-p}\epsilon^p\sum^{C_n^p}\mathbf{S}(\mathrm{Per}[\overbrace{(1-\epsilon)\cdots(1-\epsilon)}^{n-p}\overbrace{\epsilon\cdots\epsilon}^{p}])$$

$$\times f'(x_{n-1}(i_{n-1}))f'(x_{n-2}(i_{n-2}))\cdots f'(x_1(i_1))f'(x_0(i_0))\delta x_0(i),$$

$$\delta x_n(i+n)=\epsilon^n\prod_{k=0}^{n-1} f'(x_k(i+k))\delta x_0(i), \tag{A3}$$

.

the others are zero where $\mathbf{S}(\mathrm{Per}[\overbrace{(1-\epsilon)\cdots(1-\epsilon)}^{n-p}\overbrace{\epsilon\cdots\epsilon}^{p}])$ is a spatial operator. It represents the site-index permutations composed of $n-p$ elements $1-\epsilon$, and p elements ϵ. C_n^p is the number of permutation combinations. For a given number of permutation combination, we assume $i_n=i+p$, then the operating rule follows.

If the kth element is $1-\epsilon$, then $i_k=i_{k+1}$, otherwise $i_k=i_{k+1}-1$.

For example, we take $n=4,p=3$, then $C_4^3=4$. According to the above rule, we have

$$(1-\epsilon)\epsilon\epsilon\epsilon:\quad f'(x_3(i+3))f'(x_2(i+2))f'(x_1(i+1))f'(x_0(i)),$$

$$\epsilon(1-\epsilon)\epsilon\epsilon:\quad f'(x_3(i+2))f'(x_2(i+2))f'(x_1(i+1))f'(x_0(i)),$$

$$\epsilon\epsilon(1-\epsilon)\epsilon:\quad f'(x_3(i+2))f'(x_2(i+1))f'(x_1(i+1))f'(x_0(i)),$$

$$\epsilon\epsilon\epsilon(1-\epsilon):\quad f'(x_3(i+2))f'(x_2(i+1))f'(x_1(i))f'(x_0(i)).$$

Therefore,

$$\delta x_4(i+3)=(1-\epsilon)\epsilon^3[f'(x_3(i+3))f'(x_2(i+2))f'(x_1(i+1))f'(x_0(i))+f'(x_3(i+2))f'(x_2(i+2))f'(x_1(i+1))f'(x_0(i))$$
$$+f'(x_3(i+2))f'(x_2(i+1))f'(x_1(i+1))f'(x_0(i))+f'(x_3(i+2))f'(x_2(i+1))f'(x_1(i))f'(x_0(i))]\delta x_0(i).$$

In general, it is rather difficult to calculate this summation. However, this summation can be analytically worked out for some special spatiotemporal patterns. We discuss the comoving Lyapunov exponent for two patterns as follows.

The first pattern is spatial homogeneous and temporal period m $(S1Tm)$, i.e., $x_n(i)\equiv x_n(j), x_{n+m}(i)=x_n(i)$. Since the space is homogeneous, each term of the summation is the same one. Thus we have

$$\delta x_n(i+[vn])=(1-\epsilon)^{n-[vn]}\epsilon^{[vn]}C_n^{[vn]}\prod_{k=0}^{m-1} f'(x_k(i))\delta x_0(i), \tag{A4}$$

where v is the disturbance propagation velocity. As $n\to\infty$, by using the stirling formula $\ln(n!)\approx n\ln(n)-n$, we obtain the comoving Lyapunov exponent

$$L(v)=\frac{1}{m}\sum_{k=1}^{m}\ln|f'(x_k)|+\ln\frac{1-\epsilon}{1-v}+v\ln\frac{\epsilon(1-v)}{v(1-\epsilon)}. \tag{A5}$$

The second pattern is the spatiotemporal period-2 state $[S2T2,(x_+x_-,x_-x_+)]$. The evolution of the small disturbance is given by

$$\delta x_n(i+[vn])=(1-\epsilon)^{n-[vn]}\epsilon^{[vn]}[f'(x_+)f'(x_-)]^{n-[vn]/2}\sum_{k=0}^{[vn]}A_k f'(x_+)^k f'(x_-)^{[vn]-k}, \tag{A6}$$

where A_k is the coefficient of the kth term. According to numerical calculation, $|f'(x_+)|$ is larger than $|f'(x_-)|$. Therefore, as $n\to\infty$, Eq. (A6) becomes

$$\delta x_n(i+[vn])\approx(1-\epsilon)^{n-[vn]}\epsilon^{[vn]}[f'(x_+)f'(x_-)]^{n-[vn]/2}A_{[vn]}f'(x_+)^{[vn]}, \tag{A7}$$

where $A_{[vn]}=C_{n+[vn]/2}^{[vn]}$. Using the stirling formula, we immediately obtain the comoving Lyapunov exponent

$$L(v)=\frac{1}{2}\ln|f'(x_+)f'(x_-)|+\frac{v}{2}\ln\left|\frac{f'(x_+)}{f'(x_-)}\right|+(1-v)\ln(1-\epsilon)+v\ln\frac{\epsilon}{v}+\frac{v}{2}\ln\frac{1-v^2}{4}+\frac{1}{2}\ln\frac{1+v}{1-v}. \tag{A8}$$

[1] K. Kaneko, Prog. Theor. Phys. **72**, 480 (1984); **74**, 1033 (1985); Physica D **23**, 436 (1986).
[2] K. Kaneko, Phys. Lett. A **125**, 25 (1987); **149**, 105 (1990); Physica D **34**, 1 (1989); **37**, 60 (1989).
[3] D. Keeler and J.D. Farmer, Physica D **23**, 413 (1986).
[4] J.P. Cruthfield and K. Kaneko, in *Directions in Chaos*, edited by Hao Bailin (World Scientific, Singapore, 1987), p. 272.
[5] J.P. Cruthfield and K. Kaneko, Phys. Rev. Lett. **60**, 2715 (1988).
[6] Zhilin Qu and Gang Hu, Phys. Rev. E **49**, 1099 (1994).
[7] Y.C. Lai and R.L. Winslow, Phys. Rev. Lett. **74**, 5208 (1995).
[8] P.M. Gade and R.E. Amritkar, Phys. Rev. E **47**, 143 (1993).
[9] J.K. John and R.E. Amritkar, Phys. Rev. E **51**, 5103 (1995).
[10] Fagen Xie, Gang Hu, and Zhilin Qu, Phys. Rev. E **52**, R1265 (1995).
[11] K. Kaneko, Phys. Lett. A **111**, 321 (1985).
[12] R.J. Deissler and K. Kaneko, Phys. Lett. A **119**, 397 (1987).
[13] K. Kaneko, Phys. Lett. A **170**, 210 (1992).
[14] F.H. Willeboordse, Chaos **2(3)**, 423 (1992).
[15] F.H. Willeboordse and K. Kaneko, Phys. Rev. Lett. **73**, 533 (1994).
[16] F.H. Willeboordse and K. Kaneko, Phys. Rev. E **52**, 1516 (1995).
[17] K. Ohtsuka and K. Ikeda, Phys. Rev. A **39**, 5209 (1989).
[18] K.R. Sreenivasan, in *Frontiers in Fluid Mechanics*, edited by S.H. Pavis and J.L. Lumley (Springer, New York, 1985).